Polyelectrolyte Adsorption on Solid Surfaces: Theoretical Predictions and Experimental Measurements

Xie, Fei; Nylander, Tommy; Piculell, Lennart; Utsel, Simon; Wagberg, Lars; Åkesson, Torbjörn; Forsman, Jan

Published in:
Langmuir

DOI:
10.1021/la4020702

2013

Polyelectrolyte adsorption on solid surfaces: theoretical predictions and experimental measurements

Fei Xie*, Tommy Nylander**, Lennart Piculell**, Simon Utsel***, Lars Wågberg***, Torbjörn Åkesson* and Jan Forsman*

*Theoretical Chemistry, Lund University, P.O.Box 124, S-221 00 Lund, Sweden

**Physical Chemistry, Lund University, P.O.Box 124, S-221 00 Lund, Sweden

***Wallenberg Wood Science Center, KTH Royal Institute of Technology, S-100 44 Stockholm, Sweden

E-mail: fei.xie@teokem.lu.se

Abstract

This work utilizes a combination of theory and experiments, to explore the adsorption of two different cationic polyelectrolytes onto oppositely charged silica surfaces, at pH 9. Both polymers, Poly(diallyldimethylammonium chloride), PDADMAC, and Poly(4-vinyl N-methylpyridinium iodide), PVNP, are highly charged, and highly soluble in water. Another important aspect is that a silica surface carries a relatively high surface charge density, at this pH level. This means that we have specifically chosen to investigate adsorption under conditions where electrostatics can be expected to dominate the interactions. Of specific focus in this work is the response of the adsorption to the addition of simple salt, i.e. a process

*To whom correspondence should be addressed

where electrostatics is gradually screened out. Theoretical predictions from a recently developed correlation-corrected classical density functional theory for polyelectrolytes, are evaluated by direct quantitative comparisons with corresponding experimental data, as obtained by ellipsometry measurements. We find that, at low concentrations of simple salt, the adsorption increases with ionic strength, reaching a maximum at intermediate levels (about 200 mM). The adsorption then drops, but retains a finite level even at very high salt concentrations, indicating the presence of non-electrostatic contributions to the adsorption. In the theoretical treatment, the strength of this relatively modest, but otherwise largely unknown, non-electrostatic surface affinity, was estimated by matching predicted and experimental *slopes* of adsorption curves at high ionic strength. Given these estimates for the non-electrostatic part, experimental adsorption data are essentially captured with quantitative accuracy by the classical density functional theory.

Introduction

Polyelectrolytes find many applications in colloid science, some of which utilize the strong propensity of polyions to adsorb at oppositely charged particles or surfaces. We consider polyions that are oppositely charged to the surfaces or particles present in the system. The affinity of such polyions for surfaces to which they are adsorbing is so strong that they will overcompensate ("overcharge") the charge of an oppositely charged surface, immersed in a bulk solution. This has important implications to the interactions between charged particles, or surfaces, in solution.[1–5] The overcharging generates an electric double layer free energy barrier at long range, while bridging and ion correlations mediate a strong attraction at short separations. The free energy barrier can be reduced, or eliminated, by the addition of simple salt. Particularly efficient in this respect are salts including multivalent ions of the same charge as the surfaces.[5] In a pure mean-field treatment, multivalent ions will not adsorb strong enough to overcompensate the bare surface charge (in absence of any non-electrostatic surface affinity). The is simply because the mean-field attraction vanishes when the electrostatic potential drops to zero (perfect compensation). But in reality, particles with such a

high concetration of charge, are able to "pack" efficiently at the surface, and will do so in a manner that reduces their mututal repulsion below what a mean-field analysis would predict. Thus, the multivalent ion correlations facilitates high concentrations near the surface, without "too much" mutual repulsion. The net effect is that they overcompensate the bare surface charge.

The practical relevance of polyion adsorption has generated substantial theoretical[6–19] and experimental[6,16,20–32] efforts. As mentioned above, surface interactions in polyelectrolyte solutions can often be regulated by increasing or decreasing the addition of simple salt. It is thus of considerable interest to understand and predict how the adsorption of polyelectrolytes depends on the salt concentration.

Experimentally, adsorption of several kinds of polyelectrolytes to different type of surfaces have been studied, using various techniques. Hierrezuelo *et al.*[30] investigated the thickness of PDADMAC and linear PEI, adsorbed on oppositely charged sulfate latex particles, using dynamic light scattering. They found that the adsorbed layer thickness was insensitive to ionic strength at low salt concentrations, but increased significantly with ionic strength at higher salt concentrations. Seyrek *et al.*[32] used the same technique to study how the layer thickness depends on molecular mass. They found that the layer grows with polymer size at high salt, whereas this dependence is very weak at low ionic strengths. M*észá*ros et al.[22,33] used reflectometry to analyze how the adsorption of branched PEI on silica vary with pH, at low ionic strengths. PEI as well as silica are expected to titrate in the investigated interval. The authors found that the adsorption of PEI increases with pH. Furthermore, at a fixed pH, the adsorption increased with ionic strength. Adsorption of a cationic, but rather weakly charged, polyacrylamide on silica was studied by Shubin and Linse, using ellipsometry. They found that the adsorbed amount is constant at low salt concentrations, and decreases with ionic strength at high levels. They also found cation-specific effects. Liufu *et al.*[24] focused on the adsorption of MPTMAC on silica nanoparticles in aqueous solution, in the presence of different types of electrolytes and salt concentration. They found that the adsorbed amount displays a maximum as a function of salt concentration. Enarsson *et al.*[28] and Saarinen *et al.*[29] also observed this behaviour, when they studied the adsorption of CPAM on

cellulose fibers and silica surfaces. A similar trend was established by Hansupalak *et al.*[23] results, who measured the adsorbed amount of DMAEMA on silica, as a function of ionic strength at various pH values. When Rojas[34] et al. investigated adsorption of a polymer with a low linear charge density, onto an highly charged mica surface, they noted a monotonic desorption upon the addition of salt.

It is quite obvious that there is no general concensus regarding the way in which polyelectrolyte adsorption changes with ionic strength. One important reson is most likely that the charge density of the polymer and/or the surface, in many cases is relatively low. It is not uncommon, in the above reported works, to use copolymers, in which only a tiny fraction of the monomers are charged. In other cases the monomers titrate, and tend to be almost neutral at the high pH levels where the surface (usually silica) is considerably charged. These considerations imply that in many of the previous studies, polymer adsorption is influenced, but perhaps not dominated, by electrostatic interactions, at least at low ionic strength. In this work, we shall make attempts to amplify electrostatic effects, "purifying" these mechanisms as much as "possible". To this end, we shall use two different highly charged and non-titrating polymers. In other words, essentially all monomers carry a unit positive charge, protected against titration, as it is brought about by a quartenary ammonium group. This protection allows us to work at a high pH, where the silica has a substantial (negative) surface charge density. By using two different kinds of polyelectrolytes, with adsorption measurements extending to such high ionic strengths that the electrostatic interaxctions are almost entirely screenet out, we can also extract some information about the role of non-electrostatic surface affinity.

Theoretical approaches to polyelectrolyte adsorption are generally based on a mean-field approach. In absence of non-electrostatic surface affinity (i.e. pure "electrosorption" conditions), these theories tend to predict an essentially monotonic desorption, as the concentration of simple salt increases. However, by comparisons with rather extensive simulations, we have recently shown[5] that this is a qualitatively erroneous prediction. This can be directly traced to the neglect of ion correlations. Nevertheless, we showed that even a rather crude estimate of these correlations

suffice to remedy the problem, and the correlation-corrected classical polymer density functional theory, with which we compared our results, produced adsorption predictions with an almost quantitative accuracy.

In this work, we shall use this theory to predict how the adsorption of highly charged polyions at a silica surface varies with the concentration of simple salt. We shall compare these predictions with data from ellipsometry measurements, using two different polyelectrolytes:

- Poly(diallyldimethylammonium chloride), PDADMAC
- Poly(4-vinyl N-methylpyridinium iodide), PVNP

These polyions have a similar, and high, linear charge density, and are soluble in water to relatively highly concentrations. We shall demonstrate that the theory captures their overall adsorption behavior, even under the assumption that the adsorption is of purely electrostatic origin. However, a nearly quantitative agreement is obtained, for both polymers, if a short-ranged non-electrostatic surface affinity is added in the theoretical treatment.

We will first describe the experimental part of this study, followed by a rather thorough theoretical investigation, scrutinizing theory and model parameters.

Experimental Section

Materials

Polyelectrolytes. Two highly charged cationic polyelectrolytes were used in this study. Their chemical structures are illustrated in Figure 1. PVNP (Polymer Source Inc. Quebec H9P 2X8, Canada) has a reported (supplier data) average degree of polymerization of about 220. The polydispersity index (PDI) is 1.2, according to the supplier. PDADMAC (Sigma Aldrich Co.LLC) has a weight-average molar mass of 400-500kDa, but with no information on polydispersity from the supplier. Polyelectrolyte stock solutions were prepared at a monomer concentration of 2mM. Milli-Q water was used to dissolve the polyelectrolytes.

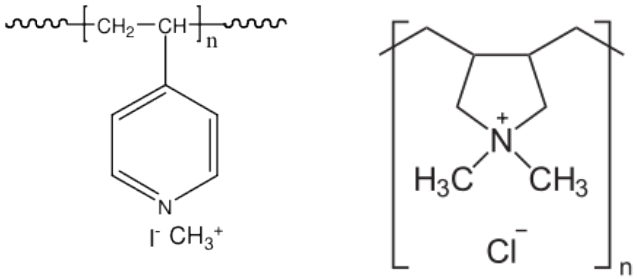

Figure 1: Chemical structure of PVNP (left) and PDADMAC (right)

Silica substrates. Silicon wafers (Semiconductor Wafer, Inc. No.3, Lane 80, Sanmin Road, Taiwan, one side polished, p-doped with boron) were used as substrate for adsorption study. The wafers have thermal oxide layer (SiO_2 layer) with a layer thickness of 300Å. The circular shapes wafers were cut into small pieces (roughly $1cm \times 3cm$ rectangular shape), and cleaned according to the following procedure:

1. A side holder, carrying rectangular pieces of silica, was placed, during 5 minutes, in a beaker containing a mixture of 160mL water, 30mL NH_3 and 30mL H_2O_2, at a temperature of 80°C.

2. The samples were rinsed by water twice, then placed (10 min) in a solution 160mL water, 30mL HCl and 30mL H_2O_2, also at 80°C.

3. The samples were rinsed twice with water, then ethanol, and finally stored in 99.7% pure ethanol.

4. Prior to ellipsometry measurements, the slides were immersed in 1mM NaOH solution for 40 min. The substrates were then rinsed with water/ethanol/water sequence, dried by nitrogen gas, and immediately placed in a Plasma cleaner (Model PDC-3XG, Harrick Scientific Corp.) for 5 min. In the latter case, the residual air was kept at 0.03 mbar, and the power consumption was adjusted to 30 W.

Buffer. Tris(hydroxymethyl) aminomethane (Tris) (Amersham LIFE SCIENCE, 26111, Miles Road, Cleveland, Ohio, USA), was used to buffer the solution around a pH value of 9 ± 0.02.

Salt solution. The Tris buffer (1mM) was prepared with different concentrations of sodium chloride (NaCl) (Sigma Chemical Co., USA. The reported purity is above 99.5%.

Polyelectrolyte solution PVNP (powder) was dissolved in buffered salt solutions, to form stock solutions with a monomer concentration of 2mM. The stock solutions were diluted 10 times, as they were added to the ellipsometry measuring cell. PDADMAC (solution) was diluted to 10g/L solution, and dialyzed for 24h, using a dialysis bag with a molecular weight cut off of 10 kDa. Specifically, 30mL of the 10g/L PDADMAC solution was placed in the dialysis bag, and the bag was immersed in 1L of Milli-Q water. This bulk water solution was replaced once, during the 24h dialysis process. PDADMAC stock solution was then prepared and added to the measuring cell the in same manner as PVNP, ensuring identical final monomer concentrations.

Methods

Refractometer. An abbe refractometer (Abbe 60/ED) was used to determine the refractive index increment (dn/dc) for the two polyelectrolytes, by measuring the refractive index (RI) of polyelectrolytes, at various concentrations, in Tris-buffered NaCl solutions. The RI was measured for different wavelengths (579.0 nm, 546.1 nm, 435.8 nm) at 25°C. The RI at 401.5 nm (ellipsometer value) was then estimated from the the Cauchy equation:[35]

$$n(\lambda) = A + B/\lambda^2 \tag{1}$$

where A and B are material constants.

Ellipsometry.

An automated Rudolph Research thin-film null ellipsomter (43603-200E) was used to measure the adsorption of the polyelectrolytes on the prepared silica surfaces. The method is based on measurements of the change of polarized light in terms of the relative phase shift, Δ, and the relative change in amplitude, Ψ, upon reflection against an interface.[36] Based on these data and optical properties of the substrate, the refractive index, n_f, and the film thickness, d_f, of the deposited

layer can be determined.[37,38] The absorbed amount (Γ) was calculated using the approach of de Feijter et. al:[39]

$$\Gamma = c * d \tag{2}$$

$$n_s - n_0 = c\frac{dn}{dc} \tag{3}$$

where n_s is the refractive index of the adsorption layer, n_0 is the refractive index of the salt solution, while dn/dc is the refractive index increment (determined as described above). The dn/dc value for PVNP with iodide is 0.176 ml/g, PVNP with chloride is 0.28, PDADMAC with chloride is 0.175 ml/g. Details about the refractive index increment measurements are provided in the Supporting Material. The influence of the silicon oxide layer is accounted for, using the methods suggested by Landgren and Jönsson.[40]

All measurements were conducted at a wavelength of 401.5nm, with an incident angle of 67.87°. The experiments were performed in situ at a temperature of 25°C, using a 5mL trapezoid cuvette made of optical glass and fitted with a magnetic stirrer, rotating at a speed of 300 rpm. The instrument allowed recording Ψ and Δ as a function of time. Every third second after injecting stock salt solution, Ψ and Δ were monitored until a horizontal and steady base line was obtained. The polymer stock solution (0.5 mL) was then injected, reaching the final desired concentration. The adsorption was then monitored, during at least 1h, or until a stable plateau value was established.[41,42]

Examples of how the measured adsorption varies with time, are provided in Figure 2 (more examples see Supporting Material). We find stable and clear plateau adsorption values, although there is some inevitable noise. The existence of a plateau is crucial, since we wish to establish how the equilibrium (infinite time) adsorption responds to changes of the (simple) salt concentration.

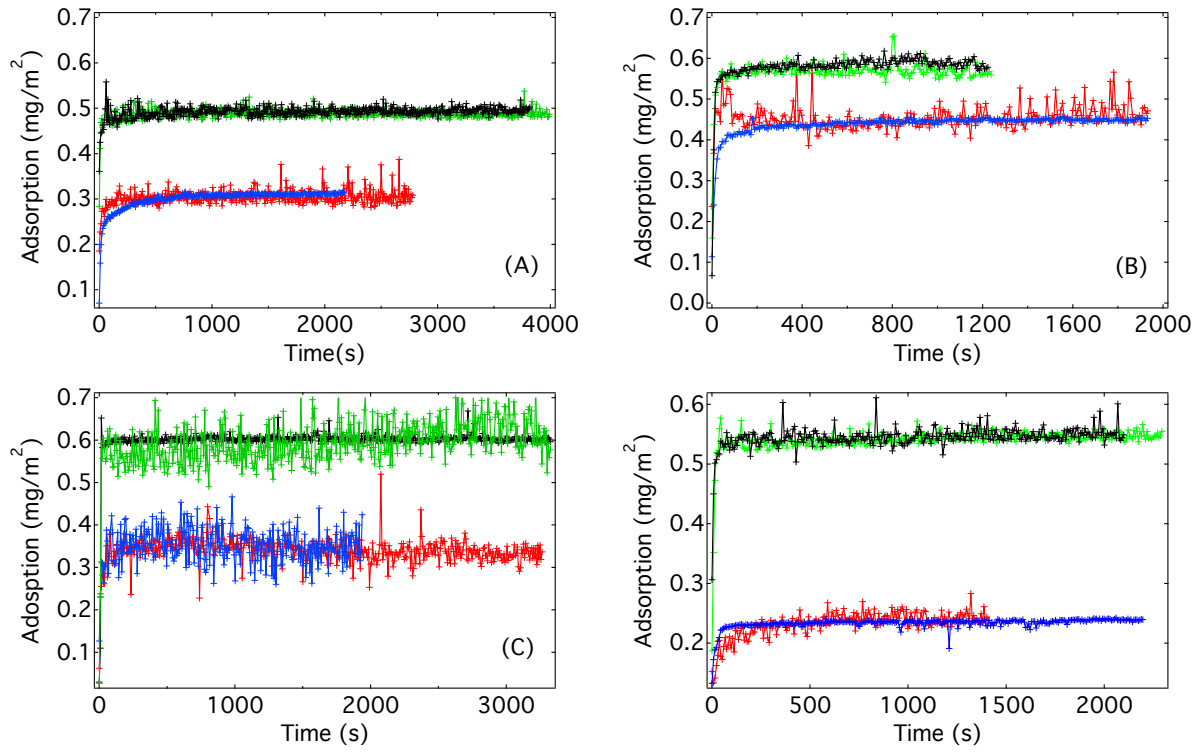

Figure 2: Adsorbed amount of PVNP and PDADMAC on silica surface as a function of time at different NaCl concentration (A:,10mM, B:80mM, C:400mM, D:1000mM) at pH 9. Green and black curves show two reproducible measurements for PVNP, while blue and red curves are for PDADMAC.

Theoretical considerations

Classical density functional theory

Here, we provide a brief and rather general recapitulation of Woodward's classical density functional theory[43] (DFT). Subsequent work has provided important extensions to this theory,[44–49] some of which will be utilized in this work.

Consider a polymer made up of q connected beads. Each of these may constitute a monomer (repeating unit), but a monomer can also contain a number of such beads. Denoting the coordinate of bead i by $\mathbf{r}_i$, we can represent a polymer configuration by $\mathbf{R} = (\mathbf{r}_1, ..., \mathbf{r}_q)$. We define a multi-point density distribution $N(\mathbf{R})$, such that $N(\mathbf{R})d\mathbf{R}$ is the number of polymer molecules having configurations between $\mathbf{R}$ and $\mathbf{R} + d\mathbf{R}$. The beads are connected by bonds, described by the bonding potential $V_b(\mathbf{R})$. In this study, we will only consider bonds of fixed length, i.e.: $e^{-\beta V_b(\mathbf{R})} \propto \prod \delta(|\mathbf{r}_{i+1} - \mathbf{r}_i| - d)$ where d is the bond length, $\delta(x)$ is the Dirac delta function, and $\beta = 1/(k_B T)$ is the inverse thermal energy. We let $\mathscr{F}_p^{id}$ denote the free energy functional for a solution containing ideal polymers, with no bead-bead interactions, save the connecting bonds. In the presence of an external field, V_{ex}, acting on all beads, this functional is *exactly* given by:[43]

$$\beta \mathscr{F}_p^{(id)} = \int N(\mathbf{R}) \left(\ln[N(\mathbf{R})] - 1\right) d\mathbf{R} + \beta \int N(\mathbf{R}) V_b(\mathbf{R}) d\mathbf{R} + \beta \int n_m(\mathbf{r} V_{ex}(\mathbf{r}) d\mathbf{r} \tag{4}$$

where $n_m(\mathbf{r})$ is the bead density (we save the index "b" for "bulk"). Interparticle interactions can only be approximately accounted for. We shall by $\mathscr{F}^{(ex)}[n_m(\mathbf{r})]$ denote the part of the functional that handles these interactions. This "excess" part is further divided into an excluded volume (hard-sphere) term, $\mathscr{F}_{HS}^{(ex)}[n_m(\mathbf{r})]$ and a separate term, $\mathscr{U}[n_m(\mathbf{r})]$, that describes bead-bead interactions at long range (the "soft" part). These contributions are added to the ideal free energy to give the total free energy $\mathscr{F}$. Our surface-adsorbing solution is naturally in equilibrium with a bulk solution, of some prescribed chemical potential (or, equivalently, bulk concentration), μ_p. In summary, the

total grand potential, Ω, has the following general appearance:

$$\Omega = \mathscr{F}^{(id)} + \mathscr{F}_{HS}^{(ex)} + \mathscr{U} - \mu_p \int N(\mathbf{R}) d(\mathbf{R}) \tag{5}$$

The exposition thus far is quite general. We shall investigate several different versions and extensions, facilitating tests of how sensitive the predicted adsorption is to various aspects of the model used. Examples of such extensions is intrinsic chain stiffness, polydispersity and polymer architecture. The excluded volume functional, $\mathscr{F}_{HS}^{(ex)}[n_m(\mathbf{r})]$, that we have chosen to use in this work, is in most cases based on the "Generalized Flory-Dimer" approach, suggested by Hall and co-workers.[50] The detailed manner in which this is incorporated into DFT has been described elsewhere,[44,47] and will not be presented here. The relevance of this part of the total functional will also be evaluated in this work, via comparisons with results obtained using a different choice.

Soft interactions, and the correlation-correction

All interactions between charged species are screened by (implicit) monovalent salt, as estimated by the Debye-Hückel screening length, κ^{-1}: $\kappa^2 = 2\frac{\beta c_S e^2}{\varepsilon_r \varepsilon_0}$, where c_S is the bulk concentration of monovalent simple salt, e is the elementary charge, ε_0 is the dielectric permittivity of vacuum, and $\varepsilon_r = 78.3$ is the (uniform) dielectric constant of the implicit aqueous solvent. Electrostatic interactions between charged beads, u_{mm}, are given by:

$$\beta u_{mm} = \frac{l_B e^{-\kappa r}}{r} \tag{6}$$

where r is the separation between the beads. All simulations and calculations were performed at a temperature of $T = 298$ K, so the Bjerrum length, l_B, is about 7.16 Å.

Previous works[5,19] have demonstrated that ion-ion correlations have to be (approximately) accounted for by the theory, else it will fail to capture important adsorption (or surface interaction) behaviors, even *qualitatively*. The importance of correlations are also highlighted by an example in the Supporting Material. Fortunately, even a rather crude estimate of these correlations will nor-

mally suffice. We shall use an approach that was recently suggested by Forsman and Nordholm.[5] Numerous direct comparisons with simulation results,[5,19] have shown that it leads to remarkably accurate predictions. We first note that mean-field expression amounts to an overcount of the interactions in the system. Consider a system with a pairwise additive interaction potential $\phi(r)$. The mean-field interaction energy per particle, $e_p^{(mf)}(\mathbf{r})$, can then be written as:

$$e_p^{(mf)}(\mathbf{r}) = \frac{1}{2}\int n(\mathbf{r}')\phi(|\mathbf{r}-\mathbf{r}'|)d\mathbf{r}' \tag{7}$$

where $n(\mathbf{r})$ is the density at position $\mathbf{r}$. It is obvious that this expression includes an interaction of the particle with itself. This can be corrected for in various ways, but we have chosen to introduce a "soft correlation hole", and assume an exponentially decaying radial distribution function, $g(r)$:

$$g(r) = 1 - e^{-\lambda r} \tag{8}$$

Here, λ is chosen such that one particle is excluded. We simplify things considerably if we let λ be position-independent, and determined by the bulk conditions:

$$\lambda = (8\pi n_b)^{1/3} \tag{9}$$

where n_b in our case is the bulk concentration of *charged* beads, which in the models of this study are always identical to the bulk monomer concentration [1]. A natural extension of the theory would be to allow λ to vary in space. Still, encouraged by previous tests,[5,19] we shall adhere to the present simplistic approach. This means that we can write the soft interaction part, of the functional, $\mathscr{U}$, as:

$$\beta\mathscr{U} = \frac{l_B}{2}\int n_m^{(c)}(\mathbf{r})\int n_m^{(c)}(\mathbf{r}')(1-e^{-\lambda(|\mathbf{r}-\mathbf{r}'|)})\frac{e^{-\kappa(|\mathbf{r}-\mathbf{r}'|)}}{|\mathbf{r}-\mathbf{r}'|}d\mathbf{r}'d\mathbf{r} \tag{10}$$

where we have introduced the notation $n_m^{(c)}$ for the density of *charged* beads. The bulk monomer concentration is given by the experimental conditions, i.e. n_b =0.2 mM.

[1] In cases where monomers are built up by several beads, only one of these will carry a unit charge

The silica surface

The adsorbing silica surface, which in our description is manifested by the external potential, V_{ex}, is modelled as a flat wall, extending infinitely in the x, y directions. The symmetry thus allows us to integrate across the x, y plane. This simplifies the free energy, making it a functional of the density distributions along the z axis.

Our reference values for the surface charge densities, σ_s, at various salt concentrations, with a silica surface at pH 9, are taken from the work by Bolt.[51] Bolt presented tabulated data for salt concentrations, c_S, of 10, 100 and 1000 mM. In order to obtain values for intermediate salt levels, we have fitted these data to an exponential expression, as illustrated in Figure 3. However, these

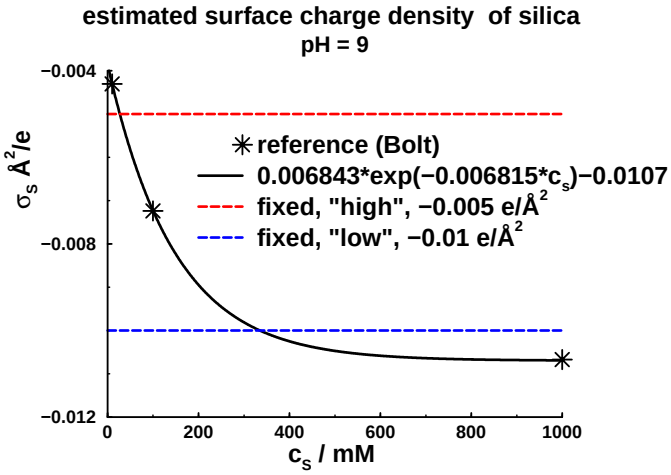

Figure 3: Surface charge density of silica at pH 9, as a function of salt concentration. Experimental data by Bolt[51] are shown as stars. The line is an exponential fit to these data: $\sigma_S \approx 0.006843e^{-0.006815c_S} - 0.0107$, where σ_S is the surface charge density, as measured in units of elementary charges per Å^2. This exponential fit provides reference values for our theoretical predictions below. However, since the actual surface charge densities of our silica wafers are rather poorly known, we shall also make comparisons (below) with theoretical predictions, using two "extreme" surface charge densities, $\sigma_S = -0.005$ ("low") $e/$Å, and -0.01 ("high") $e/$Å, respectively.

values were obtained for silical particles, the surface charge density of which might differ from those found at the silica surfaces we prepare. Unfortiunately, there are (as far as we are aware) no reported data for the salt dependence of the surface charge density, for the kind of silica surfaces that are typically used in ellipsometry. Horiuchi *et al.*[52] did investigate the charge concentration on the surface of silica wafers, but only at a salt concentration of 50 mM. The surface charge density

they measured at pH 9, essentially coincides with the corresponding value reported by Bolt, albeit at a salt concentration of just 10 mM. Hence, it is possible that our reference values are somewhat overestimated. On the other hand, one should keep in mind that the accuracy with which the charge density is determined is rather low. Hence, we shall compare adsorption predictions obtained with our reference (Bolt) values, with those obtained if a constant (salt-independent) high (-0.01 $e/\text{Å}^2$) and low (-0.005 $e/\text{Å}^2$) value, respectively, is used. These values are indicated by horizontal lines, in Figure **??**.

The (model) external potential $V_{ex}(z)$ from the silica surface, acting on the spherical beads that build up the chain, can be written as a sum of an electrostatic ($w_{el}(z)$) and a non-electrostatic ($w_s(z)$) part: $V_{ex}(z) = w_{el}(z) + w_s(z)$. The non-electrostatic part acts equally on *all* beads, i.e. charged as well as neutral. It always contains a repulsive contribution, simply modeling exchange repulsion, as the monomers approach the surface closely. As we shall see, the experimental results can only be quantitatively reproduced if we also include an attractive non-electrostatic contribution. Specifically:

$$\beta w_s(z) = \left(\frac{d}{z}\right)^6 - \gamma\left(\frac{d}{z}\right)^3 \tag{11}$$

where d is the diameter of the spherical beads that build up the chain (as well as the bond length between connected monomers). The parameter γ regulates the non-electrostatic affinity. As our reference, we have set $\gamma = 0$, i.e. pure "electrosorption". For simplicity, we shall adhere to this choice when we investigate effects from various model parameters. Thus, unless otherwise specifically stated, $\gamma = 0$.

The electrostatic contribution, which of course only acts on the charged beads, is taken from the standard Guy-Chapman model:

$$\beta w_{el} = 2\ln\left[\frac{1+\Gamma_0 e^{-\kappa z}}{1-\Gamma_0 e^{-\kappa z}}\right] \tag{12}$$

where

$$\Gamma_0 = tanh\left[\frac{\beta w_0}{4}\right] \tag{13}$$

with

$$\beta w_0 = 2sinh^{-1}\left[\frac{\sigma_S}{\sqrt{8kTc_S\varepsilon_0\varepsilon_r}}\right] \tag{14}$$

Adsorption

When the monomer distribution that minimizes the free energy functional has been established for a given set of conditions, using standard numerical methods described elsewhere,[53] we can readily calculate the net adsorption, Γ:

$$\Gamma = \int_0^\infty (n_m(z) - n_b)dz \tag{15}$$

Contrary to the model used to translate the ellipsometer output data (angles) to net adsorption, we are here not bound to assumptions of a step-wise adsorption profile. This latter assumption is an inevitable (as far as we are aware) drawback of the experimental technique. Experimental adsorption data are usually reported in units of mass/area, whereas eq.(15) provides the excess number of monomers per unit area. Thus, in order to make direct numerical comparisons with experimental data, we need to multiply by the molecular weight of a monomer. Experimental data are based upon bulk calibrations of $\partial n/\partial c$, i.e. how the refractive index changes with the monomer mass concentration. Note that the monomer mass then includes a counterion, in our case Cl^-. In principle, it would seem natural to assume that the adsorption, up to the point of surface neutralization, is provided by the positively charged monomers alone, with the counterion contributing to the "overcharging" part. However, since the full monomer+counterion molecular weight is used experimentally, it is more consistent to use the same value theoretically. As the monomer molecular weight is almost identical for the two polymers we have investigated, we shall adopt a common monomer+chloride weight of 160 g/mol.

Linear chains: a very simple polymer model

Before embarking on comparisons with experimental data, where we will adhere to a specific polymer model, it is instructive to scrutinize how sensitive the predictions are to variations of rel-

evant model parameters. In this work, we will investigate the influence of intrinsic chain stiffness, polydispersity, degree of polymerization, chain architecture, approximations of excluded volume effects, and non-electrostatic adsorption. The two first of these listed aspects are conveniently con-

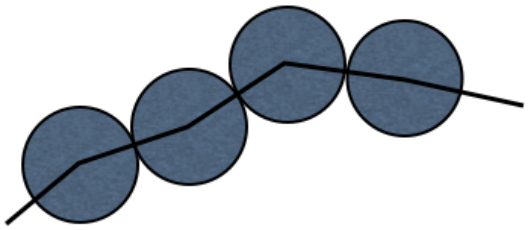

Figure 4: A simple linear model of the charged polymers. Here, all beads carry a unit charge, and have a hard-sphere diameter of 5 Å.

sidered using a simple chain architecture. We have chosen a rather standard pearl-necklace model, where all the hard-sphere beads, that constitute the monomers, have a diameter $d = 5$ Å and carry a unit charge. The model is illustrated in Figure 4.

Density profiles

At low and intermediate salt concentrations, the monomer density profile varies quite dramatically in the vicinity of the silica surface. Examples are given in Figure 5, for salt concentrations of 10 mM and 100mM. In the inset, we see that, there is a "Coulomb hole" outside the primary adsorption peak, where the monomer density is *lower* than n_b. This is particularly pronounced at 10 mM. We also note how the repulsion between adsorbed chains leads to a reduced adsorption at the lower salt concentration, despite a stronger surface attraction. This is consistent with the findings in a recent simulation + DFT study.[19]

Layer thickness

Ellipsometry rarley provide accurate measures of adsorbed layer thickness, and this quantity is not the focus of the present work. Nevertheless, it can be of some interest to briefly consider theoredical predictions of how this thickness varies with ionic strength, under electrosorption conditions (no non-electrostatic surface affinity). In principle, this should be straightforward, as we

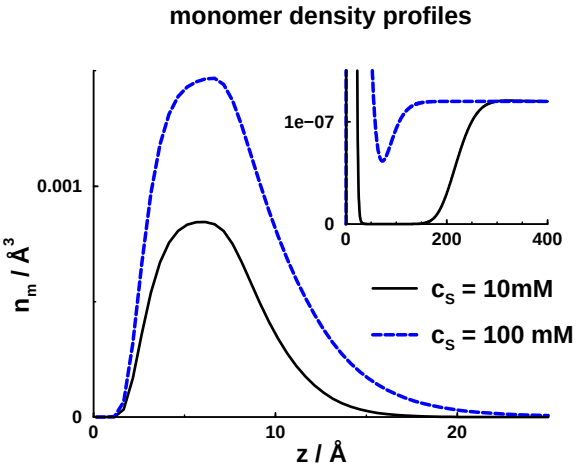

Figure 5: Monomer density profiles for the simple linear model, under pure electrosorption conditions ($\gamma = 0$), at salt concentrations of 10 and 100 mM, respectively. The inset highlights the profiles at long range. Note the difference in scale between the main graph and the inset.

have "complete knowledge" of the predicted density profile. However,layer thickness does not, in contrast to adsorption, have an unambiguous definition. Consider, for instance, the corresponding scenario under non-adsorbing conditions. Here, one typically define a "depletion thickness", $\delta \equiv \int_0^\infty (n_m(z) - n_b)/n_b dz$, which we immediately identify as Γ/n_b! In other word, if we were to use such a definition, the depletion thickness curve would have exactly the same shape as the adsorption curve (recall that the bulk monomer density, n_b is constant). However, we shall attempt to construct a definition that resembles the one we would measure with standard ellimsometry. We recall that the angles measured by the ellopsometer, are transformed to an adsorbed amount under ethe assumtion of a step-wise desnity profile. Let us try to relate the calculated (from DFT) density profile to such a step function. Specifically, we define (ambiguously) the heigh of this step profile to be identical to half the maximum height of the calulated profile (i.e. the actual profile that minimizes the grand potential). We then propose to define define the adsorbed layer thickness, Δ, such that the adsorbed amount (Γ) that would result from such a step profile, coincides with the value obtained for the full optimized profile. The resulting variation of Δ with ionic strength is presented in Figure 6. As one might have anticipated, Δ increases monotonically with added salt, and essen-

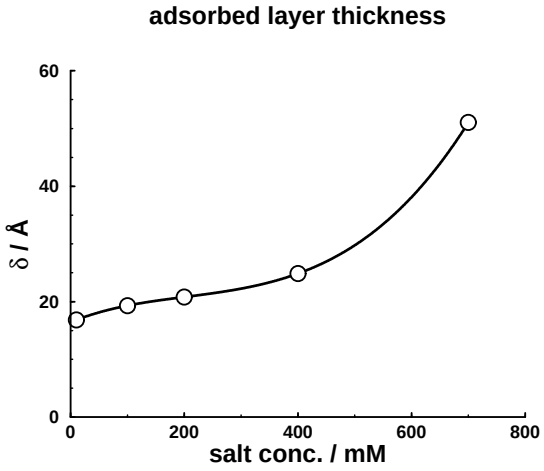

Figure 6: The variation of the adsorbed layer thickness, Δ, with salt concentration, for our simple flexible monodisperse linear polymer model, under electrosorption conditions. Our chosen definition of Δ is described in the main text.

tially diverges at very high ionic strengths (as the net adsorption vanishes, and the very concept of "layer thickness" is questionable). Given the limited accuracy with which the ellipsometer is able to estimate this quantity, we refrain from direct comparisons, but it is of interest to mention that the calculated thicknesses, in Figure 6 are in the same range as those found experimentally.

Intrinsic chain stiffness

Here we shall investigate how a bond angle potential, effectively resulting in a non-electrostatic repulsion between next-nearest neighbors along the chain, influences the net adsorption. We thus introduce a potential, E_B, defined as:

$$\beta E_B(\mathbf{s}_i, \mathbf{s}_{i+1}) = \varepsilon(1 - \frac{\mathbf{s}_i \cdot \mathbf{s}_{i+1}}{d^2}) \tag{16}$$

where, $\mathbf{s}_i$, denotes the bond vector between monomers i and $i+1$, i.e., $\mathbf{s}_i = \mathbf{r}_{i+1} - \mathbf{r}_i$, and ε is the strength of the bending potential. Thus, as ε increases, the polymers will tend to "stretch out". Physical mechanisms that may result in more stretched configurations, relative to flexible ideal chains, include (multiple) bond angle constraints and good solvent conditions. One might

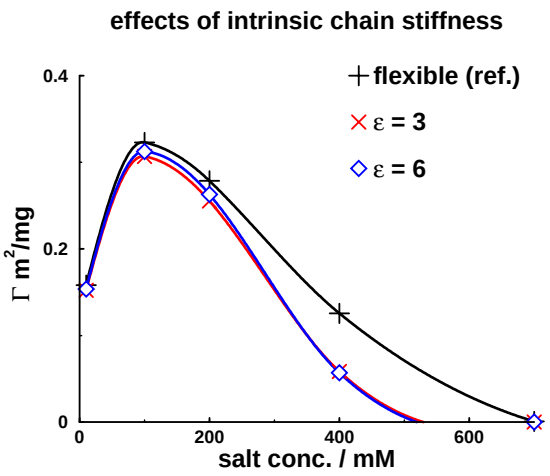

Figure 7: Comparing electrosorption curves for the linear polymer model, with different degrees of intrinsic chain stiffness, as manifested by ε (see eq. (16)).

anticipate that the intrinsic stiffness is important, but in Figure 7, we see that the effects are quite small. Recall that the monomers in this simple linear chain model should be regarded as a coarse-grained representation of several groups of atoms; thus the bond-angle potential should not be interpreted as the angular resistance of two single adjacent covalent bonds.

Polydispersity and chain length

Keeping the average degree of polymerization at 16 ("short chains") and 220 ("long chains"), respectively, we can compare DFT predictions for monodisperse and very widely polydisperse samples. Specifically, we have in the latter case assumed that the degree of polymerization, r, follows an exponential Schultz-Flory distribution:

$$F(r) = \frac{(n+1)^{n+1}}{< r >_b \Gamma(n+1)} \left(\frac{r}{< r >_b} \right)^n e^{-r\frac{n+1}{<r>_b}} \tag{17}$$

Here $\Gamma(x)$ is a gamma function and $< r >_b$ is the average degree of polymerization in the bulk. The polydispersity index, n, determines the width of the distribution, with $n = 0$ corresponding to equilibrium (living) polymers. Polymer samples displaying a Schultz-Flory distribution can be conve-

niently handled by density functional methods, as described elsewhere.[49] Here, we merely mention a remarkable feature, namely that the computational effort scales with the polydispersity index, but not the average polymer length! We will only compare the "extreme" cases of monodisperse solutions and those for which $n = 0$, the latter being simply denoted as "polydisperse". Comparisons between short and long chains, as well as monodisperse and polydisperse samples, are collected in Figure 8. Polydispersity has a rather strong influence for short average chain lengths, but is

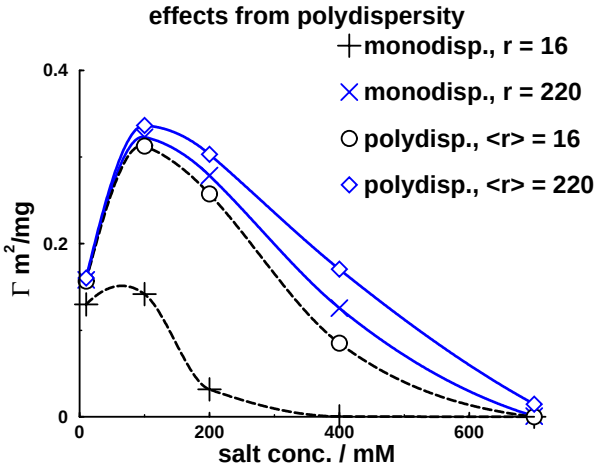

Figure 8: Electrosorption curves, for the simple linear polymer model, for different average chain lengths and polydispersity.

surprisingly unimportant for the 220-mers. In fact, the observed differences between mono-and polydisperse samples are unlikely to be larger than other inevitable experimental uncertainties. The latter include effects from surface roughness, the transformation of experimetally measured angles to adsorbed amount (assuming a step-wise density profile), and the way in which dn/dc for the polylectrolyte is used for calibration (and extrapolated to high concentrations), whereas the adsorbed layer will be enriched in the cationic monomers. These comparisons, together with results found in ref.,[19] show that:

- polydispersity can safely be neglected for average polymer lengths of a few hundred monomers, or more

- differences in chain length (between samples) can safely be neglected for average polymer lengths exceeding a few hundred monomers

These observations certainly simplifies comparisons with experimental data. Further support for the "saturation effect", in terms of chein length, beyonf $r \approx 200$, is provided in the Supporting Information.

Comb-like chains: a more elaborate polymer model

We can extend the model, to include some "flexibility" of the monomers. There are various ways to do this, the simplest of which might be to keep the simple pearl-necklace architecture, but include a few extra spheres to represent neutral parts of the monomers. Furthermore, considering the chemical structure of most polyelectrolytes, including those studied by ellipsometry in this work, it seems physically appropriate to let these extra spheres dangle out from a neutral backbone, forming a "comb-like" structure, with charged beads at the end of each side chain of the comb. The model is illustrated in Figure 9. In order to retain similar chain properties, including the overall "size" of the monomers, we must then reduce the diameter (and bond length) between the beads. Specifically, we have represented each monomer by three neutral beads, plus a charged bead. This is illustrated in Figure 9. The diameter of each bead is, somewhat arbitrarily, set to 2.5 Å, i.e. half

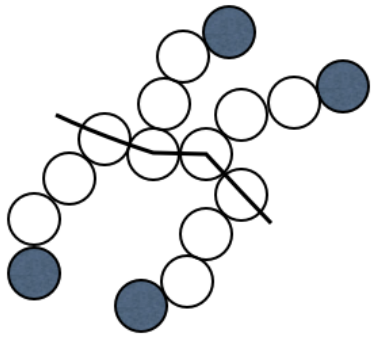

Figure 9: An illustration of a more elaborate polymer representation: the "comb polymer". Each monomer is represented by four connected hard-sphere beads, with the shaded ones (at the end of each side chain) carrying a unit charge.

the value used for the monomers of the simple linear chain.

Adsorption characteristics for our simple linear chain model, and the more elaborate comb-like version, are compared in Figure 10. The agreement is surprisingly good, suggesting that the

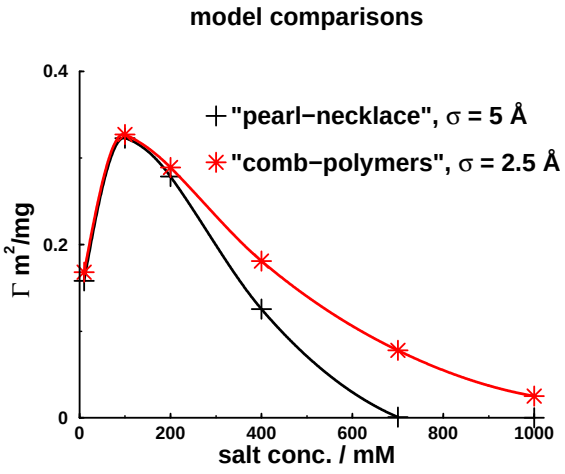

Figure 10: Comparing electrosorption curves, as obtained with the simple linear polymer model, and the corresponding "comb-polymer" model, respectively.

predictions are robust. Note, though, that the combs do adsorb more strongly at high salt. This is most likely related to the ability of smaller beads to more closely approach the surface charges. We would argue that the comb model is more realistic in this sense, but also from a broader perspective. Thus, we shall henceforth use the comb-polymer model. Finally, we note that it may be argued that, for monomers such as those in PDADMAC, it might be more realistic to place the charge at the third (rather than fourth) bead of each side chain. However, such a model will generate predictions which are almost identical to those found with the present choice. This is explicitly shown in the Supporting Material.

Surface charge density

We mentioned earlier that the actual surface charge density of our silica surfaces, is not accurately know. In Figure 11, we have investigated how sensitive the adsorption is to variations of the surface charge density. Specifically, we have compared data obtained with our reference values (taken from Bolt[51]), with a constant "high" and "low" values, respectively, as indicated by horizontal lines in

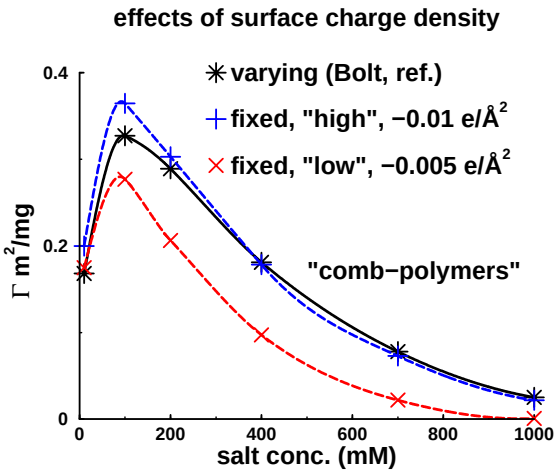

Figure 11: Electrosorption curves, as predicted using the "comb polymer" model, and various estimates of the surface charge density. Adsorption values established with our reference charge densities, taken from a fit to the values reported by Bolt,[51] are denoted by back stars. Blue and red symbols are obtained assuming constant surface charge desnities, corresponding to the (also blue and red) horizontal lines in Figure 3.

Figure 3. Our reference values produce an adsorption curve very similar to that obtained with a "high" surface charge density, indicating electrostatic saturation (at least at low salt). The "low" surface charge density, however, does result in a significant overall drop of the adsorption curve.

Excluded volume considerations

So far, excluded volume effects have been approximated by a generalized Flory-dimer (GFD) treatment, and the solvent implicitly enters via a *global* incompressibility constraint, as described by McMillan-Mayer theory. This is similar to what one would use with continuum space simulations. In a different approach, the "locally incompressible model", we enforce an overall incompressibility constraint *locally*, in the spirit of Flory-Huggins/Scheutjens-Fleer theory. Here, the implicit solvent + monomer volume fraction is fixed to a specific value at each position z outside the surface. This would be more reminiscent to a lattice type simulation, although we stress that our density functional treatment still is based on a continuum space representation. This approach leads to a different theoretical formulation, wherein the solution still can be treated as an effective one-component fluid, i.e. the solvent is incorporated implicitly. This has been thoroughly described

elsewhere.[54] Here, we merely note that our overall incompressibility constraint is formulated such that the total reduced density of beads, $n_m(z)d^3$ and implicit solvent, $n_s(z)d^3$, is always unity, i.e. $n_m(z)d^3 + n_s(z)d^3 = 1$. In Figure 12, we compare predictions from our reference GFD treatment

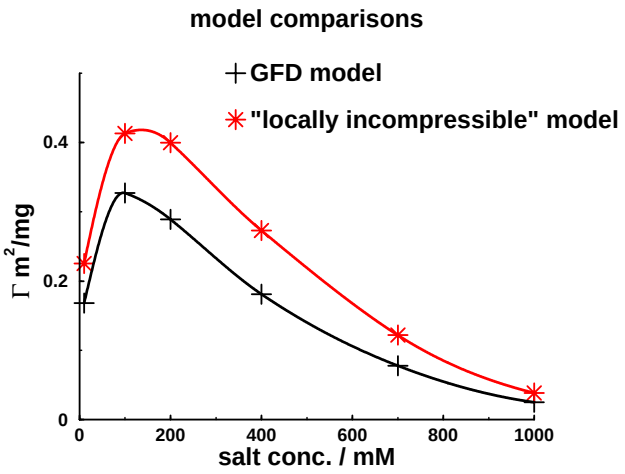

Figure 12: Electrosorption curves, as obtained by GFD and the locally incompressible model, respectively. These differ by the way in which excluded volume effects are treated (see main text).

with this "locally incompressible" version. We see that the latter model leads to stronger overall adsorption, although the shape of the adsorption curve is retained. This implies that the overall electrosorption response to salt addition is insensitive to the way in which excluded volume effects are taken into account. However, these excluded volume aspects do significantly influence the adsorption level at which the surfaces become essentially saturated. From a fundamental perspective, it is not clear which of the two alternatives considered, is more accurate. Still, the GFD treatment is our reference, and will be used for all predictions reported below. Finally, we note that the option to test various ways to estimate excluded volume effects, i.e. differnt ways to accomodate effects from the implicit solvent, is yet another advantage to the DFT approach. We are not aware of any other theoretical method that will facilitate such comparisons.

Non-electrostatic adsorption

In all the cases studied above, we have restricted ourselves to "pure electrosorption", i.e. $\gamma = 0$, in eq.(11). However, in practice non-electrostatic (by this we mean "non-ionic") contributions, due to hydrogen bonding, non-electrostatic interactions etc., is almost inevitable. Unfortunately, these are not readily established from chemical structure or physical property considerations. Fortunately, the importance and strength of these contributions can be estimated from the adsorption behavior at high salt concentrations, where the ionic contributions are expected to gradually becomes less important.

When we make direct comparisons between experiment and theory, we shall thus use non-electrostatic adsorption to make the theoretically predicted slope of Γ, as a function of salt at high concentrations, to roughly agree with the slope observed experimentally. Note that this is the *only* fitting parameter we use, given that we have established a "sensible", yet still simple, model of the polymers. Rather than quoting γ, it is more informative to use the minimum value of w_s, $w_{s,min}$, as a measure of the non-electrostatic adsorption strength. The specific w_s potentials that we have

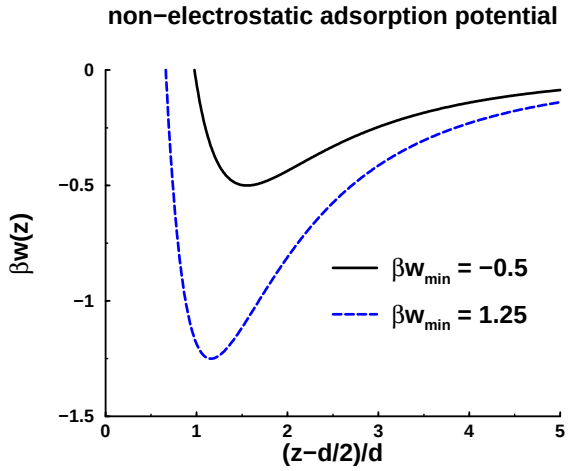

Figure 13: Illustrations of non-electrostatic contributions to the adsorption potentials. The legends indicate the maximum depth of βw_s. The values displayed are the ones that will be used below, when comparing theoretical predictions with experimental data.

used to model the experimental systems, are displayed in Figure 13. We note that these potentials

has a narrow range, only a few Å, and might thus reflect specific interactions of the kind mentioned above.

Comparisons between theory and experiments

The discussion above demonstrated that the theoretical predictions are robust, and rather insensitive to model details, except for the inclusion of ion correlations, especially at low and intermediate salt concentrations.

Our aim at the experimental part is:

- to establish how the adsorption on a silica surface, of two highly charged polymers, respond to the addition of salt
- to provide a mechanistic understanding of the adsorption process by comparing experimental results with theoretical approach, which of course also entails an evaluation of the predictive capacity of this theory

Figure 14 is a very condensed summary of the experiment results. The fact that both polymers retain a significant adsorption even at very high salt concentrations, indicate that the surface affinity is not entirely of electrostatic (by that we mean "charge-charge") origin. While we are unable to establish the detailed origin of this "extra" contribution, the higher values found for the bulkier PVNP suggest that non-electrostatic interactions are relevant. Incorporating, in an approximate and coarse-grained manner, these non-electrostatic contributions into the DFT, leads to excellent agreements between theoretical and experimental results, despite the complexity of the system. In fact, with the exception of very low salt concentrations, the agreement between theory and experimental data is essentially quantitative. The discrepancy found at low salt can have many origins, one of which is that the analyses of ellipsometer recordings (angles) do not account for any depletion layer outside the primary adsorption peak (cf. 5). Furthermore, at very low salt levels, small ionic contributions from the buffer, polymer counterions etc. may have a significant effect on the

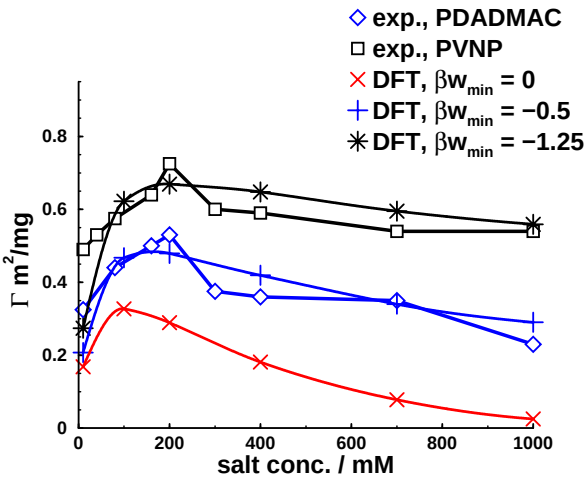

Figure 14: Comparing net adsorption of PDADMAC and PVNP, as measured by ellipsometry, and calculated by density functional theory, respectively. In the latter case, the pure electrosorption curve is also given, as reference. Values of $w_{s,min}$ are chosen so as to generate a similar slope of $\Gamma(c_S)$, at high salt concentrations (where these contributions start to dominate).

refractive index as well as on the ionic screening. These are neglected in the theoretical treatment. Finally, we note that the silica surface roughness could be of some importance, presumably producing a "true" area which is larger than the "projected" one that is seemingly studied. Including surface roughness in the theoretical tratment is beyond the scope of this study, but qualitatively we expect such extensions would lead to predictions of stronger adsorption.

Conclusion

In this work, a recently developed[5,19] correlation-corrected classical density functional theory was used to predict how the adsorption of highly charged polyions at a silica surface varies with the concentration of simple salt. By exploring a number of different polymer models, and excluded volume estimates, we have established that the theoretical predictions are remarkably robust.

According to ellipsometry data, the adsorption increases with ionic strength at low levels of simple salt, but drops at high salt concentrations. Both polymers display a residual adsorption at very high ionic strengths, suggesting that there are non-electrostatic contributions to the adsorption.

Such contributions were also added to the theoretical model, with a strength chosen so as to fit the *slope* of the experimental adsorption curves, at high salt. The agreement between theory and experimental data is essentially quantitative, except at very low ionic strengths. In the latter region, there are complicating matters, such as screening from the buffer, and a theoretically predicted depletion regime, outside the primary adsorption peak. Effects from such a regime is unlikely to be captured by the underlying simple step model, used to transform ellipsometry data (angles) to net adsorption.

References

1. Turesson, M.; Åkesson, T.; Forsman, J. Surface forces mediated by charged polymers: effects of intrinsic chain stiffness. *Langmuir* **2006**, *22*, 5734.

2. Gillies, G.; Lin, W.; Borkovec, M. Charging and Aggregation of Positively Charged Latex Particles in the Presence of Anionic Polyelectrolyte. *J. Phys. Chem. B* **2007**, *111*, 8626.

3. Turesson, M.; Åkesson, T.; Forsman, J. Interactions between charged surfaces immersed in polyelectrolyte solutions. *Langmuir* **2007**, *23*, 9555.

4. Popa, L.; Gillies, G.; Papastavrou, G.; Borkovec, M. Attractive Electrostatic Forces between Identical Colloidal Particles Induced by Adsorbed Polyelectrolytes. *J. Phys. Chem. B* **2010**, *113*, 8458.

5. Forsman, J.; Nordholm, S. Polyelectrolyte Mediated Interactions in Colloidal Dispersions: Hierarchical Screening, Simulations and a New Classical Density Functional Theory. *Langmuir* **2012**, *28*, 4069.

6. Shubin, V.; Linse, P. Effect of Electrolytes on Adsorption of Cationic Polyacrylamide on Silica: Ellipsometric Study and Theoretical Modeling. *J. Phys. Chem.* **1995**, *99*, 1285.

7. Papenhuizen, J.; van der Schee, H. A.; Fleer, G. Polyelectrolyte adsorption: I. A new lattice theory. *J. Coll. Int. Sci.* **1985**, 540.

8. Papenhuizen, J.; Fleer, B. H., G.and Bijsterbosch Polyelectrolyte adsorption: II. Comparison of experimental results for polystyrene sulfonate, adsorbed on polyoxymethylene crystals, with theoretical predictions. *J. Coll. Int. Sci.* **1985**, 553.

9. van de Steeg, H. G. M.; Cohen Stuart, M. A.; de Keizer, A.; Bijsterbosch, B. H. Polyelectrolyte adsorption: a subtle balance of forces. *Langmuir* **1992**, *8*, 2538.

10. Nordholm, S.; Rasmusson, M.; Wall, S. Simple analysis of the electrostatic screening mechanism in flocculation. *Nordic Pulp and Paper Res. J.* **1993**, *8*, 160.

11. Muthukumar, M. Adsorption of a polyelectrolyte chain to a charged surface. *The Journal of Chemical Physics* **1987**, *86*, 7230–7235.

12. Dobrynin, A. V.; Deshkovski, A.; Rubinstein, M. Theory of polyelectrolytes in solutions and at surfaces. *Macromol.* **2001**, *34*, 3421.

13. Kong, C. Y.; Muthukumar, M. Monte Carlo study of adsorption of a polyelectrolyte onto charged surfaces. *J. Chem. Phys.* **1998**, *109*, 1522.

14. Shafir, A.; Andelman, D.; Netz, R. Adsorption and depletion of polyelectrolytes from charged surfaces. *J. Chem. Phys* **2003**, *119*, 2355.

15. Netz, R.; Andelman, D. Neutral and charged polymers at interfaces. *Physics Reports* **2003**, *380*, 1.

16. Samoshina, Y.; Nylander, T.; Shubin, V.; R., B.; Eskilsson, K. *Langmuir* **2005**, *21*, 5872.

17. Carillo, J.-M. Y.; Dobrynin, A. V. Molecular Dynamics Simulations of Polyelectrolyte Adsorption. *Langmuir* **2007**, *23*, 2482.

18. Turesson, M.; Labbez, C.; Nonat, A. *Langmuir* **2011**, *27*, 13572.

19. Forsman, J. Polyelectrolyte Adsorption: Electrostatic Mechanisms and Nonmonotonic Responses to Salt Addition. *Langmuir* **2012**, *28*, 5138.

20. Lindquist, G. M.; Stratton, R. A. The role of polyelectrolyte charge density and molecular weight on the adsorption and flocculation of colloidal silica with polyethylenimine. *J. Coll. Int. Sci.* **1976**, *55*, 45.

21. Rehmet, R.; Killmann, E. Adsorption of cationic poly(diallyl-dimethyl-ammoniumchloride), poly(diallyl-dimethyl-ammoniumchloride-co-N-methyl-N-vinylactamide) and poly(N-methyl-N-vinyl-acetamide) on polystyrene latex. *Colloids and Surfaces A: Physicochemical and Engineering Aspects* **1999**, *149*, 323–328.

22. Meszaros, R.; Thompson, L.; Bos, M.; de Groot, P. Adsorption and Electrokinetic Properties of Polyethylenimine on Silica Surfaces. *Langmuir* **2002**, *18*, 6164.

23. Hansupalak, N.; Santore, M. M. Sharp Polyelectrolyte Adsorption Cutoff Induced by a Monovalent Salt. *Langmuir* **2003**, *19*, 7423–7426.

24. Liufu, S.-C.; Xiao, H.-N.; Li, Y.-P. Adsorption of cationic polyelectrolyte at the solid/liquid interface and dispersion of nanosized silica in water. *J. Coll. Int. Sci.* **2005**, *285*, 33.

25. Ondaral, S.; Wågberg, L.; Enarsson, L.-E. The adsorption of hyperbranched polymers on silicon oxide surfaces. *Journal of Colloid and Interface Science* **2006**, *301*, 32 – 39.

26. Popa, L.; Cahill, B. P.; Maroni, P.; Papastavrou, G.; Borkovec, M. *J. Coll. Int. Sci.* **2007**, *309*, 28.

27. Enarsson, L.-E.; Wågberg, L. Adsorption Kinetics of Cationic Polyelectrolytes Studied with Stagnation Point Adsorption Reflectometry and Quart z Crystal Microgravimetry. *Langmuir* **2008**, *24*, 7329–7337, PMID: 18553950.

28. Enarsson, L.-E.; Wågberg, L. Polyelectrolyte Adsorption on Thin Cellulose Films Studied with Reflectometry and Quartz Crystal Microgravimetry with Dissipation. *Biomacromolecules* **2009**, *10*, 134–141.

29. Saarinen, T.; Österberg, M.; Laine, J. Properties of Cationic Polyelectrolyte Layers Adsorbed on Silica and Cellulose Surfaces Studied by QCM-D-Effect of Polyelectrolyte Charge Density and Molecular Weight. *J. Coll. Disp. Sci.* **2009**, *30*, 969.

30. Hierrezuelo, J.; Szilagyi, I.; Vaccaro, A.; Borkovec, M. Probing Nanometer-Thick Polyelectrolyte Layers Adsorbed on Oppositely Charged Particles by Dynamic Light Scattering. *Macromol.* **2010**, *43*, 9108.

31. Jiang, M.; Popa, I.; Maroni, P.; Borkovec, M. Adsorption of poly(l-lysine) on silica probed by optical reflectometry. *Colloids and Surfaces A: Physicochemical and Engineering Aspects* **2010**, *360*, 20 – 25.

32. Seyrek, E.; Hierrezuelo, J.; Sadeghpour, A. J.; Szilagyi, I.; Borkovec, M. Molecular mass dependence of adsorbed amount and hydrodynamic thickness of polyelectrolyte layers. *Phys. Chem. Chem. Phys.* **2011**, *13*, 12716.

33. Mészáros, R.; Varga, I.; Gilányi, T. The Effect of Salt Concentration on Adsorption of Low-Charge-Density Polyelectrolytes and Interactions between Polyelectrolyte-Coated Surfaces. *Langmuir* **2004**, *20*, 5026–5029.

34. Rojas, O.; Claesson, P.; Muller, D.; Neuman, R. adsorption of poly(ethyleneimine) on silica surfaces effect of pH on the reversibility of adsorption. *Journal of colloid and interface science* **1998**, *205*, 77–88.

35. Martchenko, I. Short user manual for B+S Abbe 60/ED refractometer. **2011**,

36. R.M.A.Azzam, N. *Ellipsometry and polarized light*; ELSEVIER, 1989.

37. McCrackin, F.; Passaglia, E.; Stromberg, R.; Steinberg, H. Measurement of the thickness and refractive index of very thin films and the optical properties of surfaces by ellipsometry. *Journal of Research of the National Bureau of Standards* **1963**, *67A*, 363–377.

38. Tiberg, F.; Landgren, M. Characterization of thin nonionic surfactant films at the silica/water interface by means of ellipsometry. *Langmuir* **1993**, *9*, 927–932.

39. Feijter, J.; Benjamins, J.; Veer, F. Ellipsometry as a tool to study the adsorption behavior of synthetic and biopolymers at the air-water interface. *Biopolymers* **1978**, *17*, 1759–1772.

40. Landgren, M.; Jönsson, B. Determination of the optical properties of Si/SiO2 surfaces by means of ellipsometry, using different ambient media. *J. Phys. Chem.* **1993**, *97*, 1656–1660.

41. Equilibrium aspects of polycation adsorption on silica surface: how the adsorbed layer responds to changes in bulk solution. *Langmuir : the ACS journal of surfaces and colloids* **2005**, *21*, 5872–81.

42. Svensson, O.; Sotres, J.; Barrantes, A. Investgating protein interactions at solid surfaces-in situ, non labeling techniques.

43. Woodward, C. E. Density functional theory for inhomogeneous polymer solutions. *J. Chem. Phys.* **1991**, *94*, 3183.

44. Woodward, C. E.; Yethiraj, A. Density functional theory for inhomogeneous polymer solutions. *J. Chem. Phys.* **1994**, *100*, 3181.

45. Forsman, J.; Woodward, C. E.; Freasier, B. C. Density functional study of surface forces in athermal polymer solutions with additive hard sphere interactions: Solvent effects, capillary condensa tion, and capillary-induced surface transitions. *J. Chem. Phys.* **2002**, *117*, 1915–1926.

46. Forsman, J.; Woodward, C. E. An improved density functional description of hard sphere polymer fluids at low density. *J. Chem. Phys.* **2003**, *119*, 1889.

47. Forsman, J.; Woodward, C. E. Evaluating the accuracy of a density functional theory of polymer density functional theory of polymer solutions with additive hard sphere diameters. *J. Chem. Phys.* **2004**, *120*, 506.

48. Woodward, C. E.; Forsman, J. Density functional theory for flexible and semi-flexible polymers of infinite length. *Phys. Rev. E* **2006**, *74*, 010801.

49. Woodward, C. E.; Forsman, J. Density functional theory for polymer fluids with molecular weight polydispersity. *Phys. Rev. Lett.* **2008**, *100*, 098301.

50. Honnell, K. G.; Hall, C. K. A new equation of state for athermal chains. *J. Chem. Phys.* **1989**, *90*, 1841.

51. Bolt, G. H. Determination of the charge density of silica sols. *J. Phys. Chem.* **1957**, *61*, 1166.

52. Horiuchi, H.; Nikolov, A.; Wasan, D. T. Calculation of surface potential and surface cherge density by measurement of the three-phase contact angle. *J. Coll. Int. Sci.* **2012**, *385*, 218.

53. Forsman, J.; Woodward, C. E. Surface forces at restricted equilibrium, in solutions containing finite or infinite semi-flexible polymers. *Macromol* **2007**, *40*, 8396.

54. Forsman, J.; Woodward, C. E. Surface forces in solutions containing rigid polymers: approaching the rod limit. *Macromol.* **2006**, *39*, 1269.